Journal of Coordination Chemistry

ISSN: 0095-8972 (Print) 1029-0389 (Online) Journal homepage: http://www.tandfonline.com/loi/gcoo20

Complex formation equilibria between aluminum(III), gadolinium(III) and yttrium(III) ions and some fluoroquinolone ligands. Potentiometric and spectroscopic study

Ivan Jakovljevic, Djordje Petrovic, Ljubinka Joksovic, Ivan Lazarevic, Milena Jelikic-Stankov & Predrag Djurdjevic

To cite this article: Ivan Jakovljevic, Djordje Petrovic, Ljubinka Joksovic, Ivan Lazarevic, Milena Jelikic-Stankov & Predrag Djurdjevic (2015) Complex formation equilibria between aluminum(III), gadolinium(III) and yttrium(III) ions and some fluoroquinolone ligands. Potentiometric and spectroscopic study, Journal of Coordination Chemistry, 68:24, 4272-4295, DOI: 10.1080/00958972.2015.1089535

To link to this article: http://dx.doi.org/10.1080/00958972.2015.1089535

Journal of Coordination Chemistry, 2015
Vol. 68, No. 24, 4272–4295, http://dx.doi.org/10.1080/00958972.2015.1089535

Complex formation equilibria between aluminum(III), gadolinium(III) and yttrium(III) ions and some fluoroquinolone ligands. Potentiometric and spectroscopic study

IVAN JAKOVLJEVIC†, DJORDJE PETROVIC‡, LJUBINKA JOKSOVIC†, IVAN LAZAREVIC§, MILENA JELIKIC-STANKOV¶ and PREDRAG DJURDJEVIC*†

†Faculty of Science, University of Kragujevac, Kragujevac, Serbia
‡Laboratory for Radioisotopes, Institute of Nuclear Science "VINČA", Belgrade, Serbia
§CBRN Training Center of the Serbian Armed Forces, Kruševac, Serbia
¶Faculty of Pharmacy, Analytical Chemistry Department, University of Belgrade, Belgrade, Serbia

(*Received 12 February 2015; accepted 6 August 2015*)

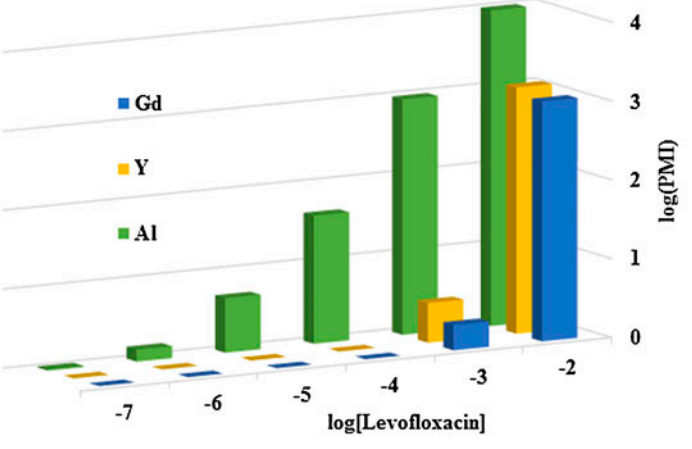

Complex formation equilibria of aluminum(III), gadolinium(III), and yttrium(III) ions with the fluoroquinolone antibacterials moxifloxacin, ofloxacin, fleroxacin, lomefloxacin, levofloxacin, and ciprofloxacin were studied in aqueous solution by potentiometric and spectroscopic methods. The identity and stability of metal–fluoroquinolone complexes were determined by analyzing potentiometric titration curves (310 K, $\mu = 0.15$ M NaCl, pH range = 2–11, $C_L/C_M = 1:1$ to $3:1$, $C_M = 1.0$ mM) with the aid of Hyperquad2006 program. The main species formed in the system may be formulated as $M_pH_qL_r$ (p = 1, q = −2 to 2, r = 1–3, L = fluoroquinolone anion, logarithm of overall stability constant, log $\beta_{p,q,r}$ = in the range *ca.* −10 to 45). The stability of complexes is mostly influenced by metal ion properties (ionization potential, ionic radius) indicating partial ionic character of the coordination bond. The complexes were also characterized by spectroscopic measurements: spectrofluorimetry, ^{1}H-NMR, and ESI-MS. Fluorimetric data were evaluated with the

*Corresponding author. Email: preki@kg.ac.rs

aid of HypSpec2014 and indicated the formation of ML_r (r = 1–3) complexes with cumulative conditional stability constants significantly lower than the thermodynamic ones. NMR and MS data corroborate potentiometrically determined speciation. Calculated plasma mobilizing capacity of the ligands generally follows the order levofloxacin > moxifloxacin > ciprofloxacin at concentration levels of the ligands higher or equal to *ca.* 10^{-4} M.

Keywords: Complexes; Aqueous equilibria; Fluoroquinolones; Aluminum; Gadolinium; Yttrium; Bio-speciation

1. Introduction

Fluoroquinolones (FQs) are synthetic antibacterial agents widely used in clinical practice for urinary and respiratory infection treatment with activity against a wide range of gram-positive and gram-negative organisms [1, 2]. FQs inhibit bacterial DNA replication enzymes but demonstrate little inhibition of human host enzymes and have an excellent safety record. Chemically, they are substituted oxo-quinoline carboxylic acids (scheme 1) and belong to the class of bidentate (O,O′) or tridentate (O,N,O′) chelating agents which exert the highest affinity toward hard Lewis acids. So, formation of very stable complexes with many divalent transition and trivalent metal ions has been observed by many researches [3–12]. Some metal–FQ complexes (complexes of ruthenium with nalidixic acid, oxolinic acid, and cinoxacin) may exhibit cytotoxic activity on some cancer cells [13]. Of particular interest is the complex formation of FQs with trivalent metal ions of diagnostic and therapeutic medical importance such as Al(III), Gd(III), and Y(III). These metal ions upon entering the human body may exhibit various toxic effects.

Aluminum is nonesential element without anyknow biological function in the organism. But it can acumulate in the human body and become of concern due to its toxicity [14–16].

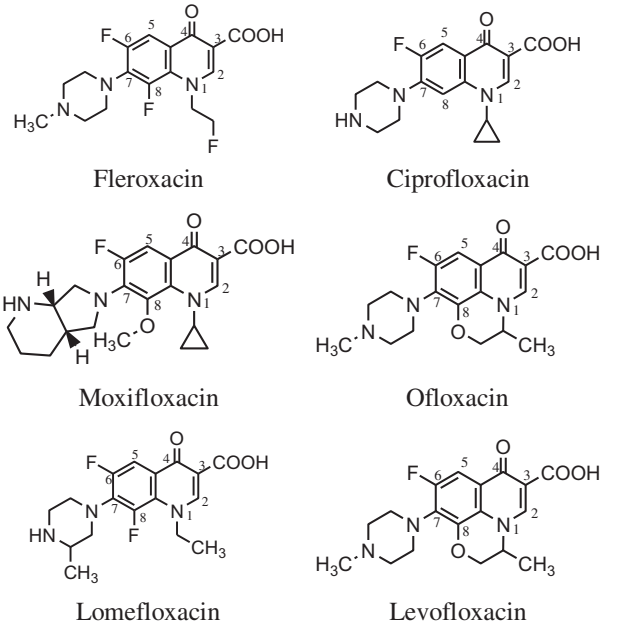

Scheme 1. Names and structures of quinolones used in this work.

Its toxicity represents a potential threat when it reaches the human body either via the environment (food, air, industrial pollution) or by medical therapy (antacids, vaccines, etc.) [17].

In the environment, yttrium is not found in large quantities (about 30 ppm), but can be dumped from petrol-producing industry and from household equipment [18–20]. In the human body, yttrium probably does not play any biological role and is not necessary for human health. ^{90}Y obtained from the ^{90}Sr–^{90}Y generator system finds widespread use in cancer treatment in the form of radiopharmaceutical chelate [21–29]. In a pure and compound form as well, yttrium is harmful and during long-term exposure may cause lung embolism and be a threat to the liver causing cancer [30, 31]. It was also found that unbound yttrium is deposited in the bones [32, 33].

In nature, gadolinium occurs together with other lanthanides. The use of gadolinium-based contrast agents increased rapidly in recent decades, consequently Gd^{3+} may be present in blood as a result of medical treatment (MRI, CT) [34]. Free gadolinium in circulation may result from similar processes as Y^{3+} ion (complex dissociation, transmetallation, ligand exchange) and it can form mineral (with OH^-, HCO_3^-, etc.) emboli in the circulation which may be deposited in tissues like muscle, skin, liver, bone, and other organs [35–39].

Fluoroquinolones, administered during parallel therapy, may complex exogenous trace metal ions and change their speciation. Complexation may change the physicochemical properties of fluoroquinolones themselves, such as solubility, bioavailability, lipophilicity, excretion, etc. Knowledge of identity, stability, and structure of metal–fluoroquinolone complexes is, thus, necessary to understand the metabolic pathway of iatrogenic trace metals and fluoroquinolones in case of parallel administration.

The complexation of aluminum(III) ion with fluoroquinolones has been intensively studied during the past two decades [4, 40–43] while gadolinium and yttrium complexation was less studied [44]. Fluoroquinolones act toward trivalent hard Lewis acids as bidentate (O,O′-donors) employing 3-carboxylate and 4-carbonyl oxygen as donors. Substituents at C-1 and C-7 positions in the quinolone core normally do not participate in coordination. In solution, numerous protonated and hydroxo species are usually formed. Formation of these species may influence fluoroquinolone behavior in biological media.

Owing to bioinorganic and biomedical importance of trace metal–fluoroquinolone interactions, in this work we characterize solution equilibria between exogenous trace trivalent metal ions with several fluoroquinolone family members using potentiometric titrations under physiological conditions. To characterize better the speciation we supplemented potentiometric measurements with some spectroscopic techniques: spectrofluorimetry, ^{1}H-NMR, and ESI-MS. These techniques should give insight into solution equilibria at micro- and nanomolar concentration levels and also into structural characteristics of complexes formed in solution.

We used computer simulation to assess the extent of the effect of fluoroquinolones on bio-speciation of trivalent metal ions, Al, Gd, and Y in blood plasma. The influence was evaluated using plasma mobilizing index (PMI) [45]. The results of the present study may be useful in understanding the biochemical pathways of trace toxic metals in the human organism and fluoroquinolone antibacterials as well. The obtained results should help to explain the FQs safety during the parallel medical therapy treatment with these antibiotics and drugs containing nonessential trivalent metal ions (antacids, contrast agents, radiopharmaceuticals, etc.). Since the computer simulations used in this work are based on the formation constant approach, we studied the complex formation of investigated metal ions with a number of fluoroquinolones by different equilibrium techniques.

2. Experimental

2.1. *Reagents*

All reagents were of analytical grade purity and used without purification. Doubly distilled water (conductivity less than 0.1 μS cm^{-1}) was used for preparation of the solutions. The stock solution of metal salts was prepared by dissolving $AlCl_3$ and YCl_3 (≥99.9% p.a., Merck, Darmstadt, FRG) in water with the addition of appropriate amount of HCl to avoid initial hydrolysis of metal ion. The stock solution of gadolinium(III) chloride was prepared by dissolving Gd_2O_3 ((≥99.9% p.a., Merck) in HCl. The concentration of metal ions was determined by EDTA complexometric titration (Titriplex Na_2-EDTA ampoule, 0.1 mol L^{-1}, Merck) [46]. The excess of HCl in the metal chloride stock solution was determined potentiometrically using Gran's method. Moxifloxacin and ciprofloxacin (declared purities > 99.9%) were obtained from Bayer Pharma AG (Berlin, Germany); ofloxacin, lomefloxacin, fleroxacin, and levofloxacin (≥99.9% purity) were purchased from Sigma Aldrich (St. Louis, MO, USA). A sodium hydroxide solution was prepared from concentrated volumetric solutions (p.a., Merck) diluted with freshly boiled doubly distilled water followed by cooling under a constant flow of purified nitrogen. The alkali concentration was checked by titration against potassium hydrogen phthalate. Hydrochloric acid solution was made from HCl "Suprapure" (Merck) and standardized against tris(hydroxymethyl)aminomethane. A sodium chloride solution was prepared from NaCl (p.a., Merck) by dissolving the recrystallized salt in doubly deionized water. The concentration of this solution was determined by evaporation of a known volume of solution to dryness at 573 K and weighing the residue. Nitrogen gas used for stirring solutions and providing an inert atmosphere during the titrations was purified by passing it through 10% NaOH and then 10% H_2SO_4, alkaline solution of pyrogallol, 0.1 mol L^{-1} solution of KCl and finally distilled water.

2.2. *Instruments*

Potentiometric measurements were made on a Tacussel Isis 20000 pH-meter (Courthezon, Vaucluse, France, precision ± 0.1 mV or ± 0.001 pH units) equipped with a Radiometer combined glass – Ag/AgCl electrode. A Metrohm (Herisau, Switzerland) Dosimat model 665 automatic burette with anti-diffusion tip was used for delivery of the titrant. Fluorescence spectra were collected on a Shimadzu RF-1501 spectrofluorimeter (Kyoto, KYT, Japan) with a 150 W Xenon lamp and 1.0 × 1.0 cm quartz cells. The slit width was set to 10 nm on both the excitation and emission monochromators. ESI MS spectra were collected on an LCQ Fleet 3D Ion Trap Mass Spectrometer (Thermo Fisher Scientific, Waltham, MA, USA). ^{1}H-NMR spectra were recorded on a Varian Gemini 200 spectrometer (Palo Alto, CA, USA).

2.3. *Procedure*

2.3.1. Potentiometric titration. All titrations were performed in the pH range from *ca.* 2–11 with constant ionic strength (μ = 0.15 M NaCl) and under purified nitrogen at 310 K. Usually stable potential readings were obtained in 1–3 min after addition of the titrant. If equilibrium could not be established within specified time interval, the point was discarded. The electrode parameters, E_0, k, and E_j from Nernst equation: $E = E_0 + k \log h + E_j$, were

determined by strong acid-strong base titrations which also served to check the system suitability. The logarithmic value of the ionic product of water was found equal to −13.21 ± 0.02. During the titrations of the test solutions the E_0 and E_j were determined using the data in the acidic region where no hydrolysis or complexation takes place (assuming that h is equal to the analytical concentration of proton), by plotting $E - k \log h$ against h and extrapolating the straight line so obtained to $h = 0$. The free proton concentration was then calculated through the equation: $\log h = (E - E_0 - E_j)/k$ and applied to the whole titration curve. All titrations were carried in duplicate. The agreement between duplicate titration was better than 1%. Molar ratios between metal ions and fluoroquinolones ($C_M : C_L$) ranged from 1 : 1 to 1 : 3 for all studied M^{3+}-FQ systems, with total metal concentration, $C_M = 1.0 \times 10^{-3}$ M.

2.3.2. Spectrofluorimetric measurements. Fluorescence spectra of FQ solutions alone (1×10^{-5} M) and FQ + metal ion, at different molar ratios ($C_M : C_{FQ} = 1 : 1$ to $100 : 1$), in TRIS buffer (2-amino-2-hydroxymethyl-propane-1,3-diol) solution (pH 7.4, 0.15 M NaCl) at 310 K were recorded. The buffer does not show fluorescence and does not complex the investigated metal ions. The concentration of the ligands was held constant, while the metal concentration was increased until no further change in spectra was observed. Excitation wavelength was chosen on the basis of the UV absorption spectra of fluoroquinolones. The UV spectra show two principal absorption bands whose maxima are situated at *ca.* 280–290 nm and *ca.* 320–340 nm [47]. The high energy band exhibits strong absorption while lower energy band is considerably weaker. The excitation wavelength was chosen at the absorption maximum of the higher energy band, since the wavelengths near the absorption maximum of the lower energy band produced too low fluorescence intensity. However, choice of excitation wavelength at 280 nm has disadvantage because it may cause an inner-filter effect so that the fluorescence intensity is not proportional to the concentration of the fluorophore [48]. It was, therefore, necessary to correct the spectra for the attenuation of the fluorescence beam (inner-filter effect).

2.3.2.1. *Consideration of the inner-filter effect.* UV absorbtion spectra demonstrate that fluoroquinolones and their metal complexes strongly absorb at 287–292 nm [47]. Thus, the intensity of the observed fluorescence may be reduced by absorption of the exciting or the fluorescence light within the tested solution and this reduction of fluorescence intensity is called the inner-filter effect. Incident light may be absorbed before it reaches the point in the sample at which fluorescence is observed and/or some of the emitted light may be re-absorbed before it leaves the cell. Because of the inner-filter effect, the observed fluorescence intensity depends on molar absorptivities of the sample at both excitation and emission wavelengths and is not a linear function of the concentration [49]. So the spectra (observed fluorescence intensities) must be corrected for the inner-filter effect. The correction factor (for right cell geometry), CF, was calculated according to Parker and Barnes equation [50]:

$$\mathrm{CF} = \frac{F_0}{F} = \frac{2.303\ A_x \Delta l_x}{10^{-A_x l_x}\left(10^{A_x \frac{\Delta l_x}{2}} - 10^{-A_x \frac{\Delta l_x}{2}}\right)} \tag{1}$$

where F_0 is the corrected fluorescence, F is the observed fluorescence, and A_x is the optical density of the solution at excitation wavelength; l_x and Δl_x are geometrical parameters of

the fluorimetric cell. The l_x, calculated according to formula $l_x = (1 - \Delta l_x)/2$. Δl_x, was set as 0.250 cm corresponding to 10 nm bandwidth. The calculated correction factor was in the range 1.15–1.23.

2.3.3. NMR measurements. All ^{1}H-NMR spectra were recorded in DMSO-d_6 and in D_2O solutions. Typical conditions for ^{1}H-NMR measurements: spectral width 3500 Hz, pulse delay time 1 s, no. of scans 72. Composition of solutions: C_M = 0.7 M; C_{FQ} = 2.0 M, pH range = 6.40–7.02.

2.3.4. ESI-MS measurements. For ESI-MS measurements, FQ-metal solutions were prepared in the FQ to metal ion concentration ratio 3 : 1 at pH 5.5 adjusted with ammonium acetate buffer. To facilitate the formation of small drops in the nebulizer and evaporation of ions, 10% (v/v) methanol was added in each solution. Concentration of fluoroquinolone in solutions was 3.0×10^{-5} M. The ESI-source parameters were as follows: source voltage 4.7 kV, capillary voltage 23 V, tube lens voltage 90 V, capillary temperature 493 K, sheath gas flow (N_2) 32 (arbitrary units). ESI-MS spectra were acquired by full range acquisition of *m/z* 100–2000.

2.3.5. Data treatment. The species formed in the studied systems were characterized by the general equilibrium:

$$pM^{3+} + qH^{+} + rL^{-} \leftrightarrow \left[M_pH_qL_r\right]^{(3p+q-r)+} \tag{2}$$

and the corresponding constants are given by:

$$\beta_{p,q,r} = \frac{\left[M_pH_q(L)_r\right]}{[M]^p[H]^q[L]^r} \tag{3}$$

where L^- is the fully deprotonated molecule of the ligand (ligand anion). The concentration stability constants of complexes, $\beta_{p,q,r}$ were calculated with the aid of the suite of Hyperquad2006 [51]. In Hyperquad calculations, the identity and stability of complexes which give the best fit to the experimental data were determined by minimizing the error square sum of the potentials, U: $U = \sum w_i(E_{obs} - E_{calc})^2$, where w_i represents a statistical weight assigned to each point of the titration curve, and E_{obs} and E_{calc} refer to the measured and calculated potentials of the cell, respectively. The E_{calc} was evaluated on the basis of Nernst's equation assuming the specific speciation model and trial values for stability constants. The quality of fit was judged by usual statistical parameters: Pearson's goodness-of-fit test, χ^2, standard deviation (SD) in potential residuals, s, and total sum of squares of potential residuals, U.

2.3.6. The human blood plasma model and speciation calculation. Updated computer model of blood plasma including 9 metals, 43 ligands, and over 6100 complexes is described earlier [45, 52]. Total concentrations of all components were taken from previously published articles [52–67].

3. Results and discussion

3.1. *Potentiometric measurements*

Reactant concentrations and pH ranges used in measurements are given in table S1. Hydrolysis of metal ions was taken into account on the basis of the literature data. For Al (III), Gd(III), and Y(III) the following hydrolytic complexes were included in calculations (stability constant given in parenthesis) corrected to physiological conditions: Al(OH) (−4.67); $Al(OH)_3$ (−13.598); $Al(OH)_4$ (−23.874); $Al_3(OH)_{11}$ (−54.694); $Al_6(OH)_{15}$ (−49.398); $Al_8(OH)_{22}$ (−76.425); $Al(OH)_{3(s)}$ (−30.4); Gd(OH) (−7.96); $Gd(OH)_2$ (−15.16); $Gd(OH)_3$ (−22.16); $Gd(OH)_{3(s)}$ (−17.9); Y(OH) (−7.71); $Y(OH)_2$ (−16.42); $Y_2(OH)_2$ (−14.23); $Y_3(OH)_5$ (−37.10); $Y(OH)_{3(s)}$ (−18.81) [44, 68–72].

The protonation constants of fluoroquinolones were mostly taken from literature data [45] and in this work we measured the constants for lomefloxacin and fleroxacin only (T = 310 K, μ = 0.15 M NaCl). The potentiometric experimental data are presented as plots of the pH dependence on the fraction titrated (titration parameter), a, calculated through the formula $a = \frac{C_{NaOH}\ V_{NaOH} - V_0\ C_{HCl}}{V_0\ C_L}$, where V_0 and C_L are the initial volume and concentration of fluoroquinolone in the titrated solution. Negative values of a represent excess of strong acid (HCl). The calculated protonation constants (total 350 data points for each system) are presented in table 1. The protonation constants for other fluoroquinolones used in the calculations are given in table S2. The points below pH *ca.* 4 and higher than pH *ca.* 9.7 were excluded from calculation. The SDs in calculated constants are given in parenthesis and indicate good precision of obtained constants.

Representative titration curves of levofloxacin without and in the presence of Al(III) ion are shown in figure 1. In the presence of metal, titration curves are shifted to the right compared to fluoroquinolone alone, indicating, thus, strong complex formation in the system, especially with increasing the total molar ratio of metal ion to ligand. Slightly smaller shifts of metal + fluoroquinolone titration curves (compared to fluoroquinolone alone) were observed in the case of other metal–fluoroquinolone systems. The titration curves show the following features: (a) in all systems at lower pH, they practically coincide with the fluoroquinolone curve, (b) three buffer regions and two inflections are seen on most metal–fluoroquinolone titration curves, and (c) at different fluoroquinolone to metal concentration ratios titration curves coincide up to the first inflection and after that point begin to spread. These features of titration curves are consistent with formation of protonated complexes and subsequent titration of released protons.

In figure 2, the titration curves of Al(III)-, Gd(III)- and Y(III)-levofloxacin solutions are presented. It can be seen that all titration curves are shifted to the right in comparison to the

Table 1. Potentiometrically determined overall protonation constants of fluoroquinolone anions $\beta_{0,q,1}$, (q = 1, 2), lomefloxacin (LMFX), and fleroxacin (FLX) at T = 310 K, μ = 0.15 M NaCl. $\beta_{0,q,1} = [H_qFQ]/[H]^q[FQ]$. The constants were calculated with the aid of Hyperquad2006. SDs in calculated constants are given in parenthesis.

FQ	log β_{011}	log β_{021}
LMFX	8.71(1)	14.22(1)
FLX	8.08(1)	13.68(2)

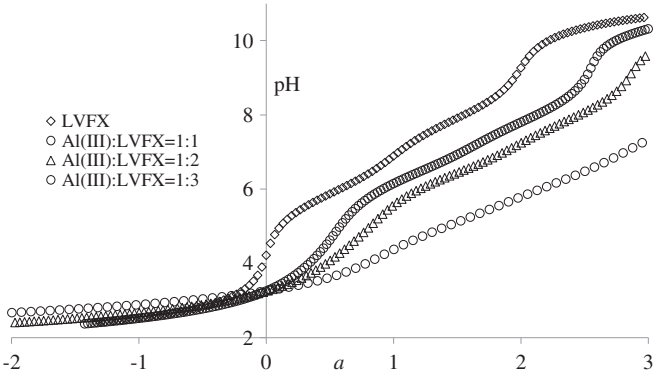

Figure 1. Potentiometric titration curves of Al(III)-LVFX solutions. C_{Al} = 1.0 M. The concentration of strong alkali (NaOH) was 0.1 M. Titration conditions: μ = 0.15 M NaCl, T = 310 K. Abscise represents the proton fraction titrated (titration parameter), a. At a = 0, proton from strong acid is titrated; at a = 1, the proton from H_2L^+ is titrated to give HL; and at a = 2, proton from HL is titrated to yield L^-.

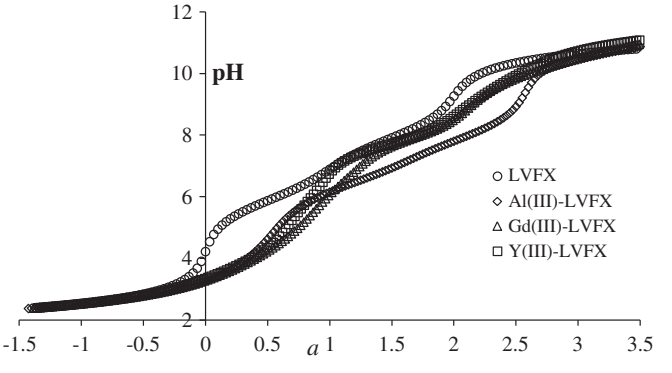

Figure 2. Potentiometric titration curves of Al(III), Gd(III), and Y(III)-LVFX solutions represented as the dependence of measured pH of solution on total proton titrated fraction (titration parameter), a. Total initial concentration of metal ion = 1.0 mM, C_{LVFX} = 3.0 mM. T = 310 K, μ = 0.15 M NaCl.

one for levofloxacin alone. The magnitude of the shift is the highest for Al, smaller for Gd, and moderate for Y. Some overlapping at the beginning of the titration is also seen. The magnitude of pH depression of metal–ligand titration curve relative to the titration of the ligand alone roughly reflects the stability of the formed complexes so it may be expected that complexes of Al will have higher stability constants than those of Gd(III) and Y(III).

Stoichiometries of possible complexes were deduced from protonation, deprotonation, and formation curves, respectively, representing:

$$\bar{J} = \frac{C_H + C_L - C_{OH} + [OH] - [H]}{C_L} \quad (4)$$

and

$$\overline{Q} = \left(C_{\mathrm{H}}^{*} - C_{\mathrm{H}}\right)/C_{\mathrm{M}} \tag{5}$$

$$\left(\text{with } C_{\mathrm{H}}^{*} = [\mathrm{H}] - [\mathrm{OH}] + \sum \mathrm{j}\left[\mathrm{LH_j}\right]\right)$$

as a function of –log [H], and

$$\overline{n} = \frac{C_{\mathrm{L}} - [\mathrm{L}]\left(1 + \sum \beta_{\mathrm{LH_j}}[\mathrm{H}]^{\mathrm{j}}\right)}{C_{\mathrm{M}}} \tag{6}$$

with $[\mathrm{L}] = \frac{C_{\mathrm{H}} - [\mathrm{H}] + [\mathrm{OH}]}{\sum \beta_{\mathrm{LH_j}}[\mathrm{H}]^{\mathrm{j}}}$, as a function of – log [L], as described by Murray and May [73].

Representative formation curves for the aluminum-levofloxacin system are shown in figure 3. In all studied systems, formation curves show small initial spread, then around $\bar{n} \sim 1$ they coincide and at n higher than 1 they spread again. Average ligand number higher than one indicates the formation of protonated complexes meaning that species like ML and ML_2H predominate or ML_2H forms in parallel with higher protonated species. For formation curves with average ligand number between 1.5 and 2, the species ML_2H and ML_2 may form. Values ≥ 2 indicate formation of ML_3 in parallel with mixed hydrolytic complexes.

The stability constants were calculated with Hyperquad2006 suite of programs [49]. To find the model that gives the best fit to the experimental data, various complexes and combinations thereof were included in calculations. During the calculations, the analytical parameters (total metal, ligand, and proton concentration) were held constant. The stability constants of the binary hydrolytic complexes and protonation constants of fluoroquinolone anion species were always fixed in calculations. We started the calculations by treatment of each titration curve separately (preliminary calculation). The results of the calculations may be summarized as follows: (a) no polynuclear complexes were accepted in any combination, (b) stability constants for MLH_2, MLH, ML, and ML_2 were always calculated for equilibrium models tested at all concentration ratios used, (c) the species ML_3, ML_3H, ML_3H_2, and ML_3H_3 were accepted only at concentration ratio $C_L/C_M = 3$, and (d) species MLH_{-1} and ML_2H_{-1} were accepted at $C_L/C_M = 2$ and 3 with relatively high SD; in other cases they

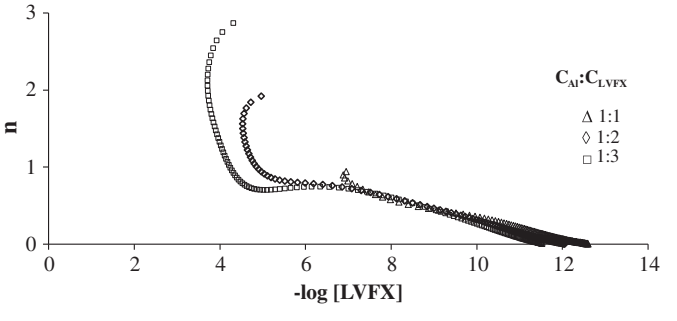

Figure 3. Formation curves for Al(III)–LVFX system. $C_{Al} = 1.0$ mM, $C_{LVFX} = 3.0$ mM.

were rejected. When we restricted the pH interval between pH 2–5, the species ML_2H_2 and ML_2H were accepted in all models. We concluded that the species MLH_2, MLH, ML, ML_2H_2, ML_2H, and ML_2 form insignificant amounts in all tested systems. In subsequent calculations, we included the points from all titration curves. Simultaneous refinement of β_{pqr} values of all species found in preliminary calculation was initiated in order to examine several models and select the "best" one. The "best" model is assumed to be a subset of the "basis" set (pqr quite general within preliminary established stoichiometries). In a first calculation cycle, the calculated set of statistics was not satisfactory and automated model selector was invoked. Some constants were either negative or excessive and were subsequently discarded. Further calculation cycles produced acceptable values for log β_{101}, log β_{111}, and log β_{121}, so that we marked these constants as "fixed" and repeated the calculations taking into account the complete "basis" set of constants. Additional constants, mostly for protonated species, were accepted. Simulation calculations with preliminary set of constants revealed the dominance of MHL, ML, and MH_2L complexes at pH values higher than 4. Therefore, points at lower pH values were excluded from calculations and at pH higher than 9.5 as well. Analyzing the results we concluded that stability constants for MLH_2, MLH, ML, MLH_{-1}, ML_2H_2, ML_2H, ML_2, ML_3H_3, ML_3H_2, ML_3H, and ML_3 are always calculated with acceptable SDs and statistical parameters of the fit. The species ML_2H_{-2} and M_2LH and all other polynuclear species were rejected in all equilibrium models and were not considered further. Some intermediate results of calculations in Al-levofloxacin system are given in table S3. Final decision on acceptance of the particular model was made taking into account absolute error in potential and volume readings. Though the precision of the potentiometer was 0.1 mV, total error was estimated according to reference [74] and taken as 0.5 mV. The error in volume readings, on the basis of the calibration of auto-burette, was 0.005 mL. These values were used in estimating the total standard error of measurements. On the basis of the statistical parameters of the fit (χ^2 – Pearson's statistics and s – SDs in potential residuals) the "best" model was chosen amongst several possible (see table S3) as the one which produced the most acceptable statistical parameters of the fit.

Calculated overall stability constants of the studied metals with some fluoroquinolones are given in table 2. Present results for complexation of studied trivalent ions with fluoroquinolones are in agreement with published data [40–44, 75–87]. Al(III)-FQ complex formation equilibria were studied previously under different conditions and methods in a number of works including those by our research group [41, 42, 87]. In this work, we determined formation constants of several Al(III)-FQ systems under physiological conditions (310 K, ionic strength 0.15 M NaCl, L/M ≥ 3). Generally, aluminum ion and fluoroquinolones form mainly complexes $Al(HFQ)_3$ or $(AlH_3(FQ)_3)$ and $Al(FQ)(HFQ)_2$ or $(AlH_2(FQ)_3)$ around physiological pH. This is in agreement with the majority of published articles. Overall stability constants of FQs with these trivalent metal ions follow the order Al > Gd > Y.

Solution equilibria in Y(III)-FQ systems were not studied previously as well as in Gd-FQ systems (except Gd(III)-moxifloxacin [44] and Gd(III)-levofloxacin [88], but not under physiological conditions). Thus, the formation constants and speciation in these systems were first determined in this work. Inspection of table 2 reveals that the dominant complexes in Y(III)-FQ systems are $Y(HFQ)_2$ or (YH_2FQ_2) and $Y(FQ)_3$ at physiological pH values. In Gd(III)-FQ systems, the dominant complexes are $Gd(HFQ)_3$ or (GdH_3FQ_3), $Gd(FQ)(HFQ)_2$ or (GdH_2FQ_3) and $Gd(FQ)_3$ under physiological conditions.

Table 2. Calculated overall stability constants log β_{pqr} (SD in parenthesis) for complexation of Al(III), Gd(III), and Y(III) ions with fluoroquinolone ($M_pH_qFQ_r$) at physiological conditions (T = 310 K, μ = 0.15 M NaCl).

	Al(III)-FQ systems					
p q r	MOX	OFLX	LVFX	CPFX	LMFX	FLX
1 2 1	−2.02(2)	−3.46(1)	−0.21(3)	–	−2.03(2)	−1.41(2)
1 1 1	5.11(2)	5.23(1)	7.68(2)	4.96(1)	5.86(2)	5.42(2)
1 0 1	11.46(1)	12.17(2)	13.92(2)	11.21(1)	13.12(1)	11.52(1)
1 1 1	16.37(1)	17.44(2)	18.85(1)	16.27(1)	18.78(2)	14.11(2)
1 2 1	–	18.54(2)	21.67(1)	18.87(2)	22.79(2)	18.24(3)
1 1 2	–	7.11(3)	7.91(2)	6.89(2)	8.81(3)	–
1 0 2	17.75(2)	15.26(2)	16.65(2)	15.92(1)	17.02(1)	16.34(2)
1 1 2	24.41(2)	22.61(1)	24.29(1)	23.73(2)	25.54(2)	24.65(3)
1 2 2	29.97(1)	28.79(2)	31.23(3)	29.67(2)	23.21(2)	–
1 0 3	18.85(2)	19.06(3)	18.19(2)	19.56(2)	18.92(3)	19.13(1)
1 1 3	28.45(2)	27.29(2)	26.29(2)	27.78(2)	30.06(2)	29.31(2)
1 2 3	35.79(1)	34.63(3)	34.14(3)	36.41(3)	38.12(3)	36.42(2)
1 3 3	44.87(2)	41.09(3)	40.79(2)	43.53(3)	44.76(1)	44.86(3)
Statistic	s = 1.47	s = 1.17	s = 1.44	s = 1.05	s = 1.23	s = 1.12
	χ^2 = 11.11	χ^2 = 10.51	χ^2 = 9.21	χ^2 = 8.11	χ^2 = 11.51	χ^2 = 8.75
	Y(III)-FQ systems					
p q r	MOX	OFLX	LVFX	CPFX	LMFX	FLFX
1 1 1	14.02(1)	–	12.72(2)	13.98(1)	13.56(2)	–
1 2 2	28.20(1)	–	25.44(2)	27.35(1)	26.11(1)	–
1 1 2	18.06(2)	–	17.65(2)	16.50(2)	17.36(2)	–
1 0 2	10.57(2)	–	10.26(1)	10.80(2)	10.05(1)	–
1 1 2	–	–	1.17(2)	0.78(3)	0.75(2)	–
1 2 2	–	–	−8.82(2)	–	−9.96(3)	–
1 0 3	12.94(1)	–	–	14.87(1)	12.65(1)	–
1 1 3	22.79(3)	–	–	24.05(2)	22.17(2)	–
1 2 3	31.01(2)	–	28.34(1)	31.45(3)	29.27(3)	–
1 3 3	38.80(1)	–	36.09(1)	39.47(1)	37.46(2)	–
Statistic	s = 1.13	–	s = 1.19	s = 1.54	s = 1.32	–
	χ^2 = 11.18	–	χ^2 = 7.21	χ^2 = 8.21	χ^2 = 10.26	–
	Gd(III)-FQ systems					
p q r	MOX	OFLX	LVFX	CPFX	LMFX	FLFX
1 0 1	–	7.02(2)	–	6.70(3)	–	–
1 1 1	14.79(2)	13.31(1)	13.16(2)	13.79(2)	–	–
1 2 2	29.57(1)	25.41(1)	25.74(2)	27.6(1)	–	–
1 1 2	21.2(1)	18.14(2)	19.17(2)	19.9(1)	–	–
1 0 2	14.02(1)	11.01(1)	11.91(2)	12.77(1)	–	–
1 1 2	–	3.34(2)	3.51(2)	4.83(2)	–	–
1 2 2	–	−6.46(3)	–	–	–	–
1 3 3	43.98(1)	37.65(2)	37.74(2)	40.34(1)	–	–
1 2 3	35.18(2)	30.71(1)	31.28(2)	–	–	–
1 1 3	27.76(1)	–	21.16(2)	–	–	–
1 0 3	19.1(3)	–	15.33(2)	–	–	–
Statistic	s = 1.21	s = 1.62	s = 1.53	s = 1.32	–	–
	χ^2 = 8.51	χ^2 = 10.36	χ^2 = 8.11	χ^2 = 7.89	–	–

The magnitude of stability constants follows the order aluminum > gadolinium > yttrium. If the second cumulative stability constant (the first stability constant in some systems was either not- or ill-defined) is plotted against ionic potential (defined as the ratio between third ionization potential and ionic radius, I_3/r), fairly linear dependence is

obtained [figure S1(a)], indicating significant ionic character of the coordination bond. For comparison, the data on iron(III)-FQ complexes taken from the literature [40, 43] are also included. Ionic character of coordination bond may be explained in terms of significant polarization effect of the central ions. The order of stability is Fe > Al > Gd > Y. The effect of ligands on stability may be described in terms of number of ligands bound to central ion, acid-base properties of the ligand ($pK_{a,1}$, $pK_{a,2}$), and partition coefficient of the ligands [89]. The data in table 2 clearly show a general trend of steep increase in overall stability with increasing the number of bound ligands. Aluminum shows maximum coordination number ($N = 3$) with all fluoroquinolones. Gadolinium does not show maximum coordination with ofloxacin and ciprofloxacin while yttrium does not reach maximum coordination with levofloxacin. If log β_2 is plotted against pI (isoelectric point), a linear relation is obtained with very small slope, indicating that no significant dependence of stability of the complexes on acid-base behavior of quinolones exists [figure S1(b)]. Similarly, stability of aluminum and gadolinium complexes may be correlated with the partition coefficient of quinolones, while yttrium shows no dependence on partition coefficient [figure S1(c)]. Urbaniak and Kokot analyzed the factors that significantly influence the stability metal fluoroquinolone complexes taking into account trivalent Al and Fe and bivalent Cu, Zn, Ca, and Mg ions [40]. The analyzed factors were number of FQ ligands in the complex structure, type of metal, type of FQ, number of hydrogen or hydroxide groups substituted in the complex molecule. They found that the type of metal, the number of coordinated FQ, and the number of proton or hydroxide groups in the complex are the most influential factors. Our results are quite in accord with their data.

3.2. *Solution equilibria and distribution diagrams*

The distribution diagrams of various complexes in M(III)-FQ solutions were calculated with the aid of program HySS2009. Some diagrams are shown in figure 4. As can be seen from figure 4, in the case of complexation of aluminum with LVFX, dominating complex at lower pH values is Al(HLVFX), with the maximum concentration at pH 3. This complex may be formed via reaction of Al(III) aqua ion and LVFX cation, bearing in mind that these species predominate in the pH region 2–4.

$$Al^{3+} + H_2LVFX^{+} \rightleftarrows [Al(HLVFX)]^{3+} + H^{+}$$

The complex $Al(HLVFX)^{3+}$, upon increasing pH, binds another zwitterionic molecule of LVFX and gives the complex $Al(HLVFX)_2^{3+}$ via the reaction path:

$$[Al(HLVFX)]^{3+} + HLVFX^{0} \rightleftarrows \left[Al(HLVFX)_2\right]^{3+}$$

This complex, upon increasing the pH, binds one more LVFX ligand forming $Al(HLVFX)_3^{3+}$ with maximum concentration (75%) at pH 6. At pH values higher than 6, a protonated LVFX in $Al(HLVFX)_3^{3+}$ releases protons and gives $Al(LVFX)(HLVFX)_2^{3+}$ followed by a series of deprotonated complexes. Gradual formation of complexes probably takes place by consecutive reactions:

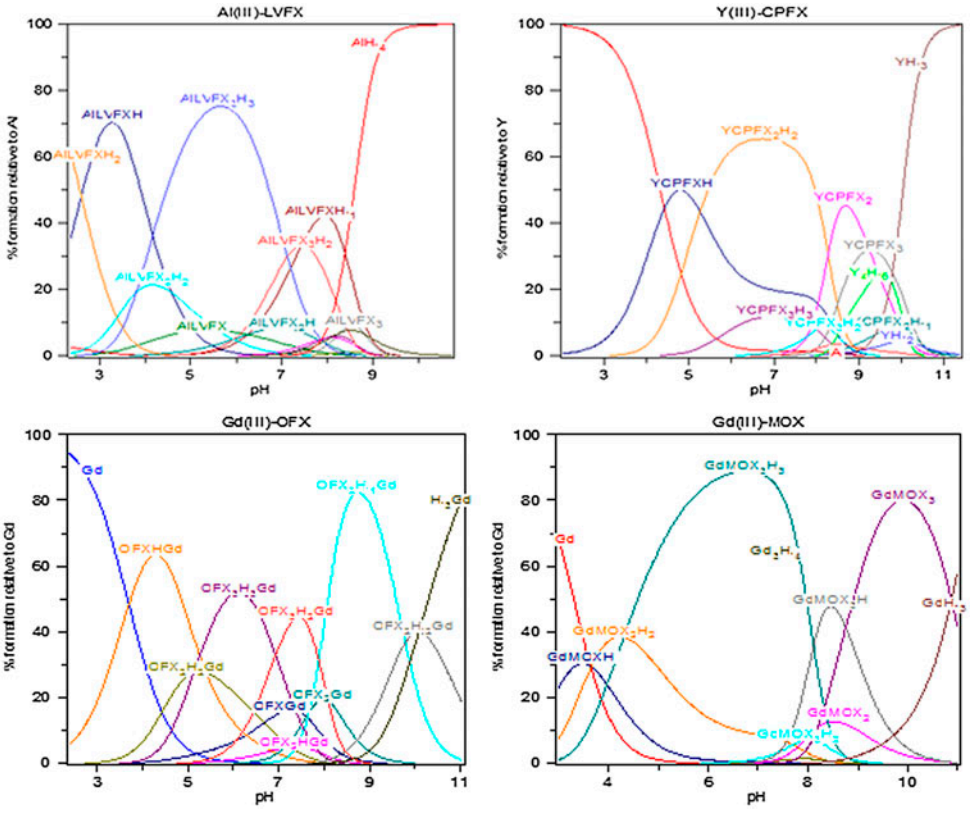

Figure 4. Distribution of species formed in Al(III)-, Gd(III)-, and Y(III)-FQ systems at ligand-to-metal concentration ratio 3 : 1 and total metal concentration 1.0 mM.

$$Al^{3+} + HLVFX^0 \rightarrow [Al(HLVFX)]^{3+} + HLVFX^0 \rightarrow [Al(HLVFX)_2]^{3+} + HLVFX^0 \rightarrow [Al(HLVFX)_3]^{3+}$$

Similar mechanism can be attributed to complexation for other Al-FQ systems. For complexation of Gd(III) with FQs similar species occur at higher pH values.

In the case of complexation of Y(III) ion with MOX, as can be seen from figure 4, the dominant species is $Y(HMOX)_2^{3+}$ with maximum concentration around physiological pH value. Upon increasing pH, the complex $Y(MOX)_3^0$ appears. This neutral complex may pass through the cell membrane causing the toxic effects or may be excreted by urinary route.

3.3. *Spectrofluorometric measurements*

Fluoroquinolones are naturally fluorescent and the intensity of fluorescence depends upon composition of medium, pH, concentration, and type of quinolone [90]. Generally, intensity of fluorescence of fluoroquinolone cation is greater than that of zwitterion.

The use of fluorescence spectroscopy to determine ligand protonation and stability constants of metal–ligand complexes depends on the difference in the fluorescence spectra

between a free acid ligand and its conjugated form and complexed ligand as well. Also the pH dependence of fluorescence spectra often does not agree with those obtained by UV–vis spectrophotometry. Fluorescence spectra depend not only on ground-state equilibria but also on excited-state proton exchange. The kinetics of the excited-state proton transfer may also influence both emission and excitation fluorescence spectra. Thus, the constants for the ground state and for the excited state can differ quite strongly. To calculate formation constants, the necessary condition is that the linear relationship between fluorescence intensity and the degree of dissociation must hold.

In spite of these difficulties, a successful determination of the ground-state protonation constants and metal stability constants of some quinolones was recently accomplished. By carefully selecting the excitation wavelength, metal and ligand total concentrations, ionic medium, and buffer the ground-state constants were estimated [91–94].

In the presence of trivalent metal ions (Mo, V, W, Al, La, Sc, Eu, Tb, Y) native fluorescence of quinolones in acidic medium is enhanced due to formation of fluorescent complex(es) [94]. In the presence of divalent metal ions (Cu, Zn, Cd, Hg, Pb, Mn), fluorescence is quenched by both dynamic and static processes in solution. In addition, ion–dipole and orbital–orbital, metal–quinolone interactions also contribute to the fluorescence quenching [93]. Chemical luminescence of fluoroquinolones in the presence of Al(III), Gd(III), and Y(III) ions was studied earlier [94], but mainly for the purpose of analytical determination of fluoroquinolones. Equilibrium constants from fluorescence data, concerning the Al(III)-, Gd(III)-, and Y(III)-FQ complexes, were not evaluated. In this work, luminiscent properties of fluoroquinolones in the presence of Al, Gd, and Y were examined using spectrofluorometric titrations technique.

Spectrofluorimetric titrations were carried out by addition of known quantities of metal ion (concentration range 0–1×10^{-3} M) to 1×10^{-5} M buffered solutions of the ligand. The wavelengths of excitation and maximum emission of FQs are listed in table 3. Fluorescence spectra of FQs in absence and presence of studied trivalent metal ions are presented in figure 5.

The addition of metal ions increases the fluorescence intensity in all Y-systems (Y-CPFX, Y-MOX, Y-LVFX), while in all Gd and Al systems fluorescence was decreased. The decrease in fluorescence is due to static reasons, i.e. complex formation between metal and zwitterionic form of FQ, $HL^{\pm}$. At pH ~ 7, the dominating form of FQ in solution is zwitterionic, HL which also has fluorescence. During complexation, its concentration decreases so the fluorescence of the solution decreases.

Fluorescence properties of FQ molecule may be utilized to measure stability constants of metal–FQ complex(es) as well as to elucidate, to some extent, the structure of the complex (es). The experimental results show that, after adding Y(III), the fluorescence intensities of CPFX increases and at the same time blue-shift of maximal emission wavelengths of CPFX is observed. In Al(III)-LVFX systems, fluorescence intensity decreases upon increasing the concentration of Al ion and then remains stable with pronounced red-shift of fluorescence maximum. Similarly, the addition of Gd(III) in MOX solution decreased the fluorescence of

Table 3. Excitation (λ^{ex}) and emision (λ^{em}) wavelengths (nm) of fluoroquinolones used for fluorescence spectral measurements.

	MOX	CPFX	LVFX
λ^{ex}	287	290	292
λ^{em}	488	450	480

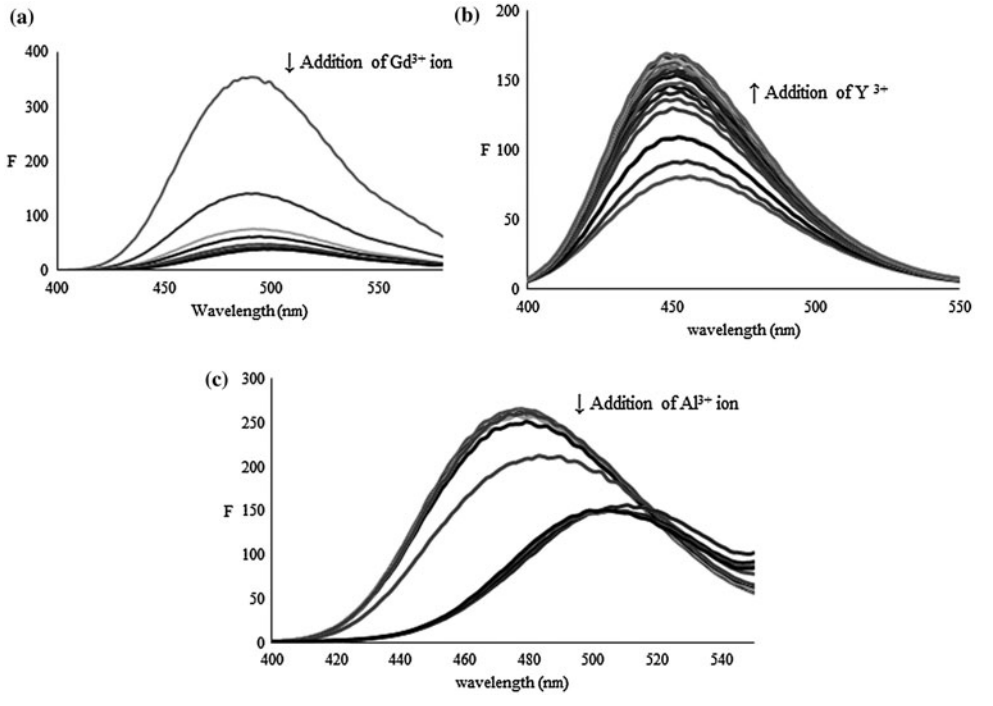

Figure 5. Fluorescence spectra of FQs ($C = 1 \times 10^{-5}$ M) in the presence of metal ions (concentration range $0–1 \times 10^{-3}$ M, pH 7.4): (a) Gd-MOX; (b) Y-CPFX; (c) Al-LVFX. F is observed fluorescence intensity corrected for inner-filter effect.

MOX with slight red-shift of fluorescence maximum. These results indicate that fluoroquinolones quickly react with metal ions to form one or more coordination compounds as $[Y(CPFX)_x]$. Due to low metal concentration in solution, it is reasonable to suppose that only mononuclear complexes with FQs are formed. The monotonic changes of the fluorescence intensity and the bathochromic shift in the spectra upon introducing the increasing metal concentrations are indicative of steady-state ground-state complex formation.

3.3.1. Stability constant determination. Fitting the whole metal–fluoroquinolone emission fluorescence spectra was performed with the aid of HypSpec2014 which belongs to the Hyperquad family of programs. The HypSpec2014 supersedes pHab program [95] for determination of equilibrium constants from spectrophotometric data and it can process UV–visible, infrared, Raman, luminescence, and fluorescence data, provided that the spectral intensity of each chemical species is proportional to the concentration of the species in solution. The spectral data may be obtained from a set of individual solutions with either known or unknown pH. Fluorescence data were processed in the wavelength interval 400–540 nm and digitized at every 1 nm. The chemical model involved general equilibrium reaction:

$$M + r(H_jL) \rightleftarrows ML_r \tag{8}$$

(j may be 0, 1, and 2)

with cumulative effective or conditional constants (β'_r) defined as the concentration quotient:

$$\beta'_r = \frac{[ML_r]}{[H_jL]^r[M]}$$

The "species" (H_jL) represents an equilibrium mixture of protonated ligand species. The conditional constant is valid only for particular experimental conditions (pH, ionic strength, temperature). The stoichiometric coefficient, r, may take integer values from 1 to 3 while j is a number of dissociable protons.

The calculated conditional constants (log β'_r) at pH 7.4 are given in table 4. Because fluoroquinolones are basic ligands, there is strong competition for protons at pH 7.4 and log β' is 6-7 orders of magnitude lower at pH 7.4 than the thermodynamic stability constant. For less basic ligands, the conditional constant is closer to the thermodynamic stability constant because there is less competition by available protons at pH 7.4. Another consequence of equation (3) is that as the pH is lowered, the concentration of protons is increased and the equilibrium in equation (3) is pushed to the left. Stronger acid conditions clearly result in lower complex stability.

To examine the fluorescence quenching mechanism a Stern–Volmer plot:

$$\frac{F_a}{F} = 1 + K_{SV}[M]$$

where F_a and F are the fluorescence intensity in the absence and the presence of the quencher, respectively, and [M] is the concentration of the metal ion constructed for Gd (III)-moxifloxacin, Al(III)-levofloxacin, and Y(III)-ciprofloxacin systems [figure S2(a–c)]. From the slope of the Stern–Volmer plot, the Stern–Volmer constant, K_{SV}, can be determined. The obtained values were: for Al-LVFX system, $K_{SV} = 9.5 \times 10^2\ M^{-1}$; for Gd-MOX system, $K_{SV} = 1.6 \times 10^2\ M^{-1}$. In Y-CPFX system, a complex fluorescence enhancing mechanism consisting of at least two steps is indicated by figure S2(c). First step is nonlinear and does not fit Stern–Volmer plot while the second step shows saturation of fluorescence intensity upon addition of Y(III) ion.

The reason for enhancement of the fluorescence and the blue-shift of the emission peak are mainly due to formation of coordination compounds. The explanation could be summarized in the following points: (1) the π–π ring conjugation plane structure in the coordination compound is enlarged in comparison with that of the free ligand, which results in enhancing of fluorescence intensity; (2) in the coordination compound, free rotation of the carboxylate or the hydroxyl of carboxylate is inhibited, which decreases the collision of inter-molecular nonradioactive energy loss; (3) shortening of the distance between Y(III)

Table 4. Calculated conditional constants from fluorimetric data for Al(III), Y(III), and Gd(III)-FQ systems (±calculated SD). The quality of fit is judged by a s-statistic.

Conditional constant	Al-LVFX	Y-CPFX	Gd-MOX
log β'_1	8.27 ± 0.02	4.73 ± 0.02	3.97 ± 0.02
log β'_2	12.60 ± 0.01	7.00 ± 0.01	9.91 ± 0.01
log β'_3	16.64 ± 0.02	11.69 ± 0.03	14.59 ± 0.02
Statistic	$s = 1.23$	$s = 0.47$	$s = 0.76$

and ligand in the coordination compound leads to positive charge transfer from Y(III) to ligand by the static action, which results in the increment of emission energy and the blue-shift of the maximal fluorescence wavelength.

3.4. *H^1-NMR measurements*

The ^{1}H-NMR spectra of yttrium complexes with LVFX in DMSO-d_6 as well as D_2O are analyzed to confirm their formation. The binding of LVFX-Y(III) was studied by changing the molar ratio of drug to metal ion as presented in figure S3. The most evident changes were observed for 5-H and 2-H protons after addition of Y(III) ions. In the ^{1}H-NMR spectrum of pure LVFX in DMSO-d_6, the singlet at 8.85 ppm was attributed to 2-H proton, while 5-H proton appeared as a doublet at 7.53 ppm due to coupling with ^{19}F nucleus. The signals due to the free drug decreased in intensity and new signals appeared as amount of Y(III) increased. When Y(III) was added (drug : Y(III) = 6 : 1), ^{1}H-NMR spectrum showed additional signals for 5-H and 2-H protons. As concentration of metal ion was increased (3 : 1), the new peaks reached 45% of total integral intensity. At 2 : 1 (drug : Y(III)), these new signals become dominant and transformed into broad singlets at 1 : 1 ratio.

The results clearly indicate that new species formed by complexation with Y(III) (drug : Y(III) = 6 : 1 and 3 : 1) have stable ligand at room temperature with slow ligand exchange between free and coordinated LVFX [96]. Broadening of 5-H and 2-H signals in the presence of increasing metal ion amount (drug : Y(III) = 2 : 1 and 1 : 1) induced by paramagnetic metal center and quadrupole effects might be an indication of a strong binding of drug to metal [97]. At the same time, by increasing concentrations of Y(III) ion, the intensity of carboxylic proton decreases and this signal completely disappears at drug : Y(III) = 2 : 1 ratio [98]. Similar changes are observed for C-15 methyl group, while the signals of other protons of coordinated LVFX are shifted to lower field. The obtained results suggest that keto and deprotonated carboxylate oxygen are identified as the metal ion binding site in LVFX complex.

The same coordination mode was observed after analysis of ^{1}H-NMR spectra of yttrium complexes with LVFX in D_2O. A subsequent addition of Y(III) ions to the solution of pure LVFX in D_2O leads to pH lowering but no new signals, except slight chemical shift to higher δ values, were detected (figure S4). However, after pH adjustment at 8.5, new signals for 5-H and 2-H protons as well as protons of two methyl groups appeared. At lower drug : Y(III) ratios, these signals broadened and finally coalesced into broad singlets at drug : Y(III) = 3 : 1 ratio (figure S5). It can be concluded that coordination of LVFX with yttrium ion in D_2O is very dependent on applied pH.

^{13}C-NMR spectra give less information on complexation than ^{1}H-NMR spectra. The signal assigned to keto carbonyl carbon at 176.5 ppm split into a complex multiplet in DMSO-d_6 after addition of Y(III) ions, whereas the same signal in D_2O does not undergo significant changes in multiplicity and chemical shift.

Similar behavior is observed for complexation of CPFX to yttrium ion in DMSO-d_6. When Y(III) was added (drug : Y(III) = 3 : 1), the ^{1}H-NMR spectrum of CPFX displayed additional signals for H-2, H-5, and H-8 protons. At ratio of drug : Y(III) = 1 : 1, the signals due to free drug decreased in intensity and new peaks for these protons were dominant in the ^{1}H-NMR spectrum, indicating the binding of drug to metal ion (figure S3). At the same time, the carboxylic proton completely disappeared at drug : metal ion = 1 : 1 ratio,

confirming the coordinated drug through carboxylate oxygen. The new signals were also detected for cyclopropane ring protons after complexation, while piperazine protons are far away from coordination center and their signals in ^{1}H-NMR spectrum underwent significantly smaller changes in comparison with free ligand.

3.5. *ESI-MS measurements*

To further confirm the speciation derived from potentiometric and fluorescence measurements ESI-MS measurements were made on fluoroquinolone-metal ion solutions. The binary metal–fluoroquinolone systems were studied to verify the speciation picture obtained by potentiometry. Some typical ESI-MS spectra for two metal–ligand systems are given in figures S6–10. The spectra were selected as representative examples of the complexity of the signals obtained. The multitude of signals corresponding to clusters of various compositions includes fluoroquinolones, protons, sodium and hydroxide ions. It was possible to characterize some potentiometrically species relative to FQ protonation and metal–FQ complexation. Table 5 reports the most salient *m/z* values corresponding to positively charged species formed in metal–FQ solutions. Molecular mass, isotopic distributions, and (in same cases) MS/MS spectra allowed unambiguous peak assignments. Experimental conditions are listed in the caption of table 5.

The extent of ESI-induced in-source fragmentation is not pronounced due to low voltages applied to extraction electrode. The fragmentation probably proceeds by collisional activation of M(FQ)H and M(FQ)H_2 ions. The fragments form mostly due to the loss of neutral molecules CO_2, NH_3, HF sometimes followed by addition of one or two molecules of water. Addition of water is a result of the presence of trace levels of water molecules in ion trap. The CO_2 molecules originate from coordinated COOH functional group. Loss of HF and NH_3 results in destruction of quinolone core, but coordination of metal ion may remain preserved due to distant coordination sites relative to fragmented bond.

The ESI-MS analysis confirms the results obtained by equilibrium techniques because the same Al(III), Gd(III), and Y(III) complexes (ML, ML_2, ML_3) were detected in the gas phase (ESI-MS is not able to discriminate differently protonated species). Several fragmentations of adduct products were observed as usual for these systems.

3.6. *Evaluation of plasma mobilizing capacity*

The normal blood plasma model used in simulation was described in our earlier articles [45, 52]. The bio-speciation of Al, Gd, and Y ions in the presence of fluoroquinolone in blood plasma was modeled using the HySS2009 program. To this model, stability constants of typical essential metal ions present in plasma with FQs are added. A complete list of complexes of components in blood plasma database and constants was described in detail in our previous work [52].

The ability of FQs to compete with plasma metal ions and with other low molecular weight ligands can be assessed in terms of the PMI proposed by May *et al*. [61]. This index can be used to define mobilization power of FQs to the metal ions in blood plasma. The PMI of a particular metal ion is defined as the ratio of the total concentration of low molecular mass (LMM)-metal species in the presence and absence of the exogenous ligand in blood plasma:

Table 5. Experimental positive mass measurements in ESI-MS analysis of Al(III), Gd(III), and Y(III)-fluoroquinolone solution at pH 5.5. ($C_{Al} = C_{Gd} = C_Y = 1.0 \times 10^{-5}$ M, $C_{FQ} = 3.0 \times 10^{-5}$ M).

Experimental (*m/z*)	Identified species/ions	Corresponding species in solution
	Y-MOX	$[Y(MOX)_r]$ (r = 1–3)
646.1	$[Y(HMOX)_2(MOX)]^{(2+)}$	
855.8	$[Y(MOX)_2–2NH_3]^+$	
889.8	$[Y(MOX)_2]^+$	
907.8	$[Y(MOX)_2 + H_2O]^+$	
1290.2	$[Y(MOX)_3]^+$	
	Y-CPFX	$[Y(CPFX)_3]$
996.9	$[Y(CPFX)_3–2HF–C_2H_2–NH_3]^+$	
1011.9	$[Y(CPFX)_3–2HF–C_2H_4]^+$	
1018.9	$[Y(CPFX)_3–CO_2–NH_3]^+$	
1051.9	$[Y(CPFX)_3Na–3NH_3]^+$	
1059.9	$[Y(CPFX)_3Na–CO_2]^+$	
1065.9	$[Y(CPFX)_3Na–HF–NH_3]^+$	
1079.9	$[Y(CPFX)_3]^+$	
1102.9	$[Y(CPFX)_3Na]^+$	
	Y-LVFX	$[Y(LVFX)_r]$ (r = 1–3)
143.8	$[Y(HLVFX)–H_2O]^{3+}$	
227.6	$[Y(LVFX)\cdot 3H_2O–CO–HF]^{2+}$	
388.3	$[Y(LVFX)(HLFX)–2NH_3]^{2+}$	
432.3	$[Y(LVFX)(HLVFX)\cdot 3H_2O]^{2+}$	
792.6	$[Y(LVFX)_2–NH_3]^+$	
1102.0	$[Y(LVFX)_3Na–3NH_3–2HF]^+$	
1190.0	$[Y(HLVFX)(LVFX)_2\cdot 2H_2O–NH_3]^+$	
	Gd-MOX	$[Gd(MOX)_r]$ (r = 1–3)
278.8	$[Gd(MOX)]^{2+}$	
453.1	$[Gd(MOX)(HMOX)–CH_4–NH_3–HF]^{2+}$	
470.6	$[Gd(MOX)(HMOX)–H_20]^{2+}$	
680.3	$[Gd(MOX)(HMOX)_2]^{2+}$	
941.1	$[Gd(MOX)_2–NH_3]^{2+}$	
	Gd-CPFX	$[Gd(CPFX)_r]$ (r = 1–3)
389.5	$[Gd(HCPFX)(CPFX)-2HF]^{2+}$	
401.5	$[Gd(HCPFX)(CPFX)–CH_4]^{2+}$	
558.6	$[Gd(HCPFX)_2(CPFX)–2NH_3]^{2+}$	
763.9	$[Gd(CPFX)_2–HF–2NH_3]^+$	
797.9	$[Gd(CPFX)_2–HF]^+$	
833.9	$[Gd(CPFX)_2 + 2H_2O–HF]^+$	
1007.3	$[Gd(CPFX)_3–2CO_2–2H_2O–NH_3]^+$	
1042	$[Gd(CPFX)_3–2CO_2–NH_3]^+$	
1104.3	$[Gd(CPFX)_3 –CO_2]^+$	
1138.3	$[Gd(CPFX)_3\cdot H_2O–C_2H_4]^+$	
1166.3	$[Gd(CPFX)_3 + H_2O]^+$	

$$\text{PMI} = \frac{\text{Total concentration of LMM} - \text{metal species in the presence of drug}}{\text{Total concentration of LMM} - \text{metal species in normal plasma}}$$

This is a useful tool to carry out preliminary *in vitro* assessment of mobilizing influence of chelating agents using computer modeling based on the thermodynamic data for the equilibria occurring in blood plasma.

In our earlier simulation studies, we found that the influence of FQs on speciation of Cu (II), Ni(II), and Zn(II) is non-significant at normal concentration levels of these ligands in

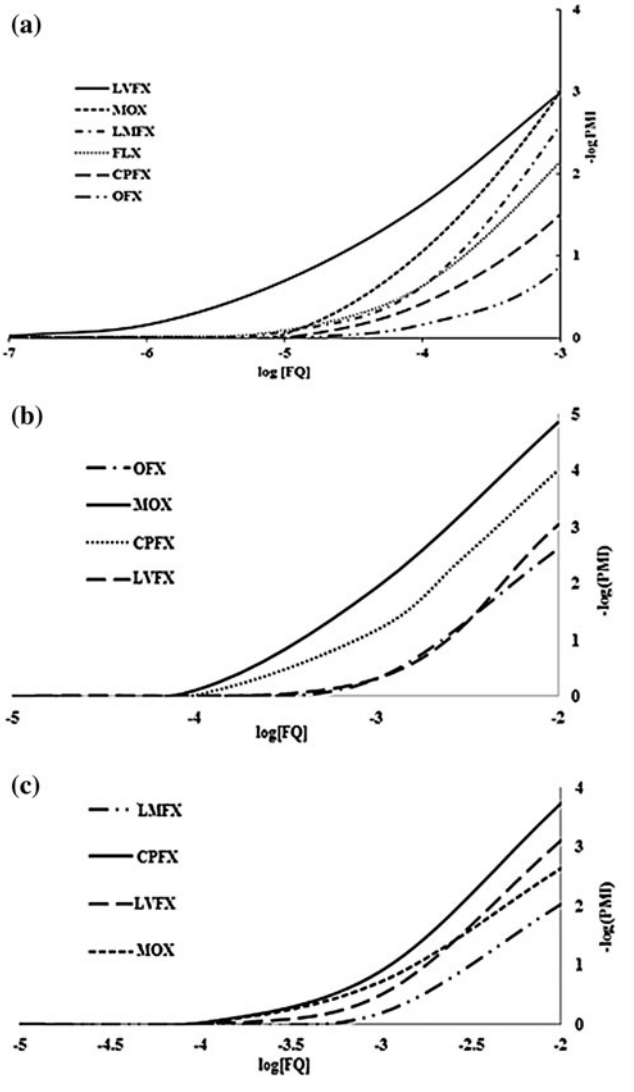

Figure 6. The effect of fluoroquinolone ligands on plasma mobilization of (a) aluminum, (b) gadolinium, and (c) yttrium.

blood plasma [45]. Literature data indicate that Al(III), Y(III), and Gd(III) readily form complexes with fluoroquinolones of medium-to-high stability. Thus, it may be expected that fluoroquinolones can affect the complicated equilibrium system: blood proteins-metal ion-LMM species in plasma in which aforementioned trace metals are involved. By competing with plasma ligands, fluoroquinolones may lower the free metal ion concentration to the extent which could cause dissociation of labile metal–protein complex leading to increase in the percentage of LMM complexes. Depending on charge of the complexes they may be either excreted or deposited in tissues. The effect of fluoroquinolones on bio-distribution of particular LMM species of nonessential trace metal ions was not studied so far.

The PMI curves of aluminum ion with studied FQs are shown in figure 6(a). Mobilization of aluminum ion by FQs does not occur at ligand concentration lower than 5×10^{-7} M. Results obtained from HySS2009 calculation indicate that FQs below the concentration of 10^{-6} M are dominantly bound into the calcium and magnesium complexes. Aluminum ion is mainly bound to the mixed ternary phosphate-citrate complex (about 65%) [52]. At higher concentration of FQs, the Al(LVFX)H_{-1} and Al(LVFX) complexes are formed. From figure 6(a), it can be seen that mobilization of Al ions is most significant with LVFX while other FQs show the order LVFX >> MOX ≈ FLX > CPFX > OFX.

Aluminum ion is not appreciably bound to serum proteins except transferrin. However, the aluminum-transferrin complex is so strong (log K_1 = 12.9, log K_2 = 12.3 [99]) that it is not possible that FQs can extract Al(III) from the Al(III)-transferrin complex. Expansion of PMI occurs at expense of Al(III) mobilization from tissue deposits. Particularly, Al(III) is deposited in kidneys lysosomes, Golgi apparatus, and mitochondria. FQs site of action are kidneys so that they, at higher concentration, could mobilize Al(III) deposits from kidney cells. The formed Al(III)-FQ complexes at pH7 are charged so that their excretion via the kidney route may be facilitated.

Mobilization of gadolinium and yttrium ions by FQs is shown in figure 6(b) and (c). The similarity in their PMI curves implies that both gadolinium and yttrium are mobilized by FQ ligands at similar degree in human blood plasma. At FQs concentration range from 1×10^{-7} to 1×10^{-4} M no significant changes in relative percentage of Gd-LMM and Y-LMM species are observed. In the presence of MOX, the concentration of major Gd-LMM species increases at ligand concentration ≥ 10^{-4} M, while CPFX shows similar effect on yttrium. Thus, these ligands at normal serum concentrations do not disturb significantly the bio-speciation of Gd(III) and Y(III) ions in blood plasma. The effects of OFX and LVFX do not differ appreciably. Relatively slow rise of PMI curves indicates that the mobilization of Gd(III) and Y(III) ions is a result of the extraction of these ions from their albumin complexes (Gd-HSA: log K_1 = 6.4 [100]). Complexes with transferrin are of similar stability (Gd-Tf: log K_1 = 6.8 [101]), so that metal sequestration with FQs is also probable.

Levofloxacin is very poor at mobilizing Gd(III) and Y(III) in blood plasma and mobilizes Al(III) ion significantly better (figure S11). Similar trend was observed for other quinolones. These ligands preferentially bind to Cu(II), Zn(II), and Fe(II) due to high stability of the complexes and much higher concentrations of essential bivalent ions in plasma than trivalent Gd(III) and Y(III). This means that they could easily displace Gd(III) and Y(III) from their complexes.

4. Conclusion

Trivalent metal ions and fluoroquinolones form *in vitro*, in aqueous solution, an array of complexes of which $M(HL)_3$ is predominant at physiological pH ($C_L/C_M \geq 3$). At millimolar level of concentration, only mononuclear complexes are formed with protonated ones being dominant at pH ≤ 5. Neutral complexes are formed at higher pH values by at least two mechanisms: (a) dissociation of protons and (b) metal ion reaction with zwitterionic forms of fluoroquinolones. ESI-MS data are in fair agreement with the speciation in solution. NMR spectra confirm the structure of complexes with 4-carbonyl and 3-carboxylate oxygens as donors. Stability of complexes is mainly dependent on metal properties and less on fluoroquinolone identity. Stabilities of complexes derived from fluorescence data

favorably compare with those from potentiometric titrations. Obtained values of equilibrium constants indicate possible mobilization capacity of the ligands toward the studied metal ions. In the case of aluminum ion, the highest mobilization effect showed LVFX even at normal administered dose (10^{-6} M) leads to increase in Al-LMM species relative percentage for 35%. The dominant species $Al(PO_4)Cit$ increases 15%. Other FQs have similar effect at concentration $\geq 10^{-5}$ M. Mobilization of gadolinium and yttrium ions by FQs occurs at ligand concentration $\geq 10^{-4}$ M. Moxifloxacin mostly influences gadolinium ion, leading to Gd-LMM species increase in 45% at ligand concentration of 10^{-4} M. Effect of CPFX is similar to the other FQs on mobilization of yttrium ion from blood plasma pool but only at 10-fold to 100-fold higher concentration than the normal serum concentration of these antibiotics.

Acknowledgements

Financial support from the Ministry of Education, Science and Technological Development of Serbia, under the project 172016, is gratefully acknowledged. We are grateful to reviewers and Associate Editor for valuable comments.

Disclosure statement

No potential conflict of interest was reported by the authors.

Funding

This work was financially supported by the Ministry of Education, Science and Technological Development of Serbia [grant number 172016].

Supplemental data

Supplemental data for this article can be accessed http://dx.doi.org/10.1080/00958972.2015.1089535.

References

[1] A.M. Emmerson, A.M. Jones. *J. Antimicrob. Chemother.*, **51**, 13 (2003).
[2] G. Sheehan. In *Fluoroquinolone Antibiotic*, A.R. Roland, D.E. Low (Eds.), pp. 1–10, Birkhauser, Basel (2003).
[3] I. Turel. *Coord. Chem. Rev.*, **232**, 27 (2002).
[4] V. Uivarosi. *Molecules*, **18**, 11153 (2013).
[5] A. Tarushi, E. Polatoglou, J. Kljun, I. Turel, G. Psomas, D. Kessissoglou. *Dalton Trans.*, **40**, 9461 (2011).
[6] G. Psomas, D. Kessissoglou. *Dalton Trans.*, **42**, 6252 (2013).
[7] A. Galani, E. Efthimiadou, T. Theodosiou, G. Kordas, A. Karaliota. *Inorg. Chim. Acta*, **423**, 52 (2014).
[8] A. Galani, E. Efthimiadou, G. Mitrikas, Y. Sanakis, V. Psycharis, C. Raptopoulou, G. Kordas, A. Karaliota. *Inorg. Chim. Acta*, **423**, 207 (2014).
[9] I. Sousa, V. Claro, J.L. Pereira, A.L. Amaral, L.C. Cunha-Silva, B. de Castro, M.J. Feio, E. Pereira, P. Gameiro. *J. Inorg. Biochem.*, **110**, 64 (2012).
[10] P. Živec, F. Perdih, I. Turel, G. Giester, G. Psomas. *J. Inorg. Biochem.*, **117**, 35 (2012).
[11] W.Y. Huang, J. Li, S.L. Kong, Z.C. Wang, H.L. Zhu. *RSC Adv.*, **4**, 35193 (2014).

[12] J.L. Zhang, J. Yang, X. Wang, H.Y. Zhang, X.L. Chi, Y. Chen, Q. Yang, D.R. Xiao. *Z. Anorg. Allg. Chem.*, **641**, 820 (2015).
[13] J. Kljun, I. Bratsos, E. Alessio, G. Psomas, U. Repnik, M. Butinar, B. Turk, I. Turel. *Inorg. Chem.*, **52**, 9039 (2013).
[14] J. Savory. *Clin. Chem.*, **40**, 1477 (1994).
[15] T.B. Drueke. *Life Chem. Rep.*, **11**, 231 (1994).
[16] R. Doll. *Age Ageing*, **22**, 138 (1993).
[17] Toxicological Profile for Aluminum. *US Department of Health and Human Services Agency for Toxic Substances and Disease Registry* (2008). Available online at: http://www.atsdr.cdc.gov.
[18] S.R. Taylor. *Geochim. Cosmochim. Acta*, **28**, 1273 (1964).
[19] A.P. Vinogradov. *Geochemistry*, **7**, 641 (1962).
[20] G. Morteam. *Eur. J. Mineral.*, **3**, 641 (1991).
[21] International Atomic Energy Agency. *Final Report of a Coordinated Research Project 1998–2002, Labelling Techniques of Biomolecules for Targeted Radiotherapy*, IAEA, Vienna, 2003.
[22.] S. Liu, D.S. Edwards. *Top. Curr. Chem.*, **222**, 259 (2002).
[23] S. Liu. *Chem. Soc. Rev.*, **33**, 1 (2004).
[24] D.E. Reichert, J.S. Lewis, C.J. Anderson. *Coord. Chem. Rev.*, **184**, 3 (1999).
[25] D.M. Goldenberg. *Crit. Rev. Oncol./Hematol.*, **39**, 195 (2001).
[26] A.J. Grillo-López. *Expert Rev. Anticancer Ther.*, **2**, 485 (2002).
[27] A.J. Davies. *Oncogene*, **26**, 3614 (2007).
[28] T.E. Witzig, A. Molina, L.I. Gordon, C. Emmanouilides, R.J. Schilder, I.W. Flinn, M. Darif, R. Macklis, K. Vo, G.A. Wiseman. *Cancer*, **109**, 1804 (2007).
[29] G. Paganelli, M. Bartolomei, C. Grana, M. Ferrari, P. Rocca, M. Chinol. *Neurol. Res.*, **28**, 518 (2006).
[30] S.A. Gulec, G. Mesoloras, W.A. Dezarn, P. McNeillie, A.S. Kennedy. *J. Transl. Med.*, **5**, 15 (2007).
[31] C.Y. Wong, M. Savin, K.M. Sherpa, F. Qing, J. Campbell, V.L. Gates. *Cancer Biother. Radiopharm.*, **21**, 305 (2006).
[32] J.S. Stewart, V. Hird, D. Snook, B. Dhokia, G. Sivolapenko, G. Hooker, J.T. Papadimitriou, G. Rowlinson, M. Sullivan, H.E. Lambert. *J. Clin. Oncol.*, **8**, 1941 (1990).
[33] W. Breeman, M. De Jong, E. De Blois, B. Bernard, M. De Jong, E. Krenning. *Nucl. Med. Biol.*, **31**, 821 (2004).
[34] M. Ferrari, M. Cremonesi, M. Bartolomei, L. Bodei, M. Chinol, M. Fiorenza, G. Tosi, G. Paganelli. *J. Nucl. Med.*, **47**, 105 (2006).
[35] M. Port, J.M. Idée, C. Medina, C. Robic, M. Sabatou, C. Corot. *BioMetals*, **21**, 469 (2008).
[36] P. Hermann, J. Kotek, V. Kubicek, I. Lukes. *Dalton Trans.*, **23**, 3027 (2008).
[37] M.A. Sieber, H. Pietsch, J. Walter, W. Haider, T. Frenzel, H. Weinmann. *Invest. Radiol.*, **43**, 65 (2008).
[38] T. Grobner, F.C. Prischl. *Kidney Int.*, **72**, 260 (2007).
[39] G. Lazar. *J. Reticuloendothel. Soc.*, **13**, 231 (1973).
[40] B. Urbaniak, Z.J. Kokot. *Anal. Chim. Acta*, **647**, 54 (2009).
[41] P. Djurdjevic, M. Jelikic-Stankov. *J. Pharm. Biomed. Anal.*, **19**, 501 (1999).
[42] P. Djurdjević, L. Joksović, R. Jelić, A. Djurdjević, M. Stankov. *Chem. Pharm. Bull.*, **55**, 1689 (2007).
[43] B. Urbaniak, Z.J. Kokot. *Acta Pol. Pharm.*, **70**, 621 (2013).
[44] P. Djurdjevic, R. Jelic, L. Joksovic, I. Lazarevic, M. Jelikic-Stankov. *Acta Chim. Slov.*, **57**, 386 (2010).
[45] P. Djurdjevic, I. Jakovljevic, L. Joksovic, N. Ivanovic, M. Jelikic-Stankov. *Molecules*, **19**, 12194 (2014).
[46] J. Bassett, R.C. Denney, G.H. Jeffery, J. Mendham. *Vogel's Textbook of Quantitative Inorganic Analysis*, 5th Edn, pp. 309–324, Longman, Essex (1989).
[47] H.R. Park, T.H. Kim, K.M. Bark. *Eur. J. Med. Chem.*, **37**, 443 (2002).
[48] C.A. Parker, W.T. Rees. *The Analyst*, **87**, 83 (1962).
[49] M. Kubista, R. Sjöback, S. Eriksson, B. Albinsson. *The Analyst*, **119**, 417 (1994).
[50] C.A. Parker, W.J. Barnes. *The Analyst*, **82**, 606 (1957).
[51] P. Gans, A. Sabatini, A. Vacca. *Talanta*, **43**, 1739 (1996).
[52] I. Jakovljevic, D. Petrovic, L. Joksovic, I. Lazarevic, P. Djurdjevic. *Acta Chim. Slov.*, **60**, 861 (2013).
[53] S. Daydé, M. Filella, G. Berthon. *J. Inorg. Biochem.*, **38**, 241 (1990).
[54] G.E. Jackson. *Polyhedron*, **9**, 163 (1990).
[55] T. Kiss, A. Lakatos, E. Kiss, R.B. Martin. In *Interaction of Al(III) with Biomolecules: Bioinorganic Chemistry and Biological Implication in Cytotoxic, Mutagenic and Carcinogenic Potential of Heavy Metals Related to Human Environment*, N.D. Hadjiliadis (Ed.), pp. 231–251, NATO ASI Series, Kluwer, Dordrecht (1997).
[56] A. Lakatos, F. Evanics, G. Dombi, R. Bartani, T. Kiss. *Eur. J. Inorg. Chem.*, **2001**, 3079 (2001).
[57] J.R. Duffield, K. Edwards, D.A. Evans, D.M. Morrish, R.A. Vobe, D.R. Williams. *J. Coord. Chem.*, **23**, 277 (1991).
[58] W.R. Harris. *Clin. Chem.*, **38**, 1809 (1992).
[59] D.J. Clevette, C. Orvig. *Polyhedron*, **9**, 151 (1990).
[60] W.R. Harris, Z. Wang, Y.Z. Hamada. *Inorg. Chem.*, **42**, 3262 (2003).

[61] P.M. May, P.W. Linder, D.R. Williams. *Experientia*, **32**, 1492 (1976).
[62] G.E. Jackson, S. Wynchank, M. Woudenberg. *Magnet. Reson. Med.*, **16**, 57 (1990).
[63] C.J.L. Silwood, M. Grootveld. *Biochim. Biophys. Acta*, **1725**, 327 (2005).
[64] K. Diem, C. Lentner. *Documenta Geigy Scientific Tables*, 7th Edn, Geigy Pharmaceuticals, Basle (1970).
[65] R.M. Smith, A.E. Martell, R.J. Motekaitis, *NIST Standard Reference Database 46, NIST Critically Selected Stability Constants of Metal Complexes Database, Version 8.0*, National Institute of Standards and Technology, Gaithersburg (2004).
[66] Stability Constants Database and Mini-SCDatabase. *IUPAC and Academic Software. Version 5.3.*, Sourby Old Farm, Timble (2003).
[67] P.M. May, K. Murray. *Talanta*, **38**, 1409 (1991).
[68] S. Dayde, V. Brumas, D. Champmartin, P. Rubini, G. Berthon. *J. Inorg. Biochem.*, **97**, 104 (2003).
[69] T. Amaya, H. Kakihana, M. Maeda. *Bull. Chem. Soc. Jpn.*, **46**, 1720 (1973).
[70] A. Shalinets, A. Stepanov. *Radiokhim.*, **14**, 280 (1972).
[71] G. Biedermann, L. Ciavatta. *Ark. Kemi.*, **22**, 253 (1964).
[72] J. Kragten, L.G.D. Decnop-Weever. *Talanta*, **27**, 1047 (1980).
[73] K. Murray, P.M. May. *ESTA, Equilibrium Simulation for Titration Analysis (Version 1.1)*, Users manual, University of Wales Institute of Science and Technology, Wales (1984).
[74] E.N. Néher-Neumann. *Advanced Potentiometry, Potentiometric Titrations and their Systematic Errors*, Springer Science and Business Media B.V., Stockholm (2009).
[75] S.C. Wallis, B.G. Charles, L.R. Gahan, L.J. Filippich, M.G. Bredhauer, P.A. Duckworth. *J. Pharm. Sci.*, **85**, 803 (1996).
[76] Y. Kawai, K. Matsubayashi, H. Hakusui. *Chem. Pharm. Bull.*, **44**, 1425 (1996).
[77] M. Nakano, M. Yamamoto, T. Arita. *Chem. Pharm. Bull.*, **26**, 1505 (1978).
[78] Y. Okabayashi, F. Hayashi, Y. Terui, T. Kitagawa. *Chem. Pharm. Bull.*, **40**, 692 (1992).
[79] M.H.S.F. Teixeira, L.F. Vilas-Boas, V.M.S. Gil, F. Teixeira. *J. Chemother.*, **7**, 126 (1995).
[80] B.M. Sánchez, M.M. Cabarga, A.S. Navarro, A.D.G. Hurlé. *Int. J. Pharm.*, **106**, 229 (1994).
[81] D.S. Lee, H.J. Han, K. Kim, W.B. Park, J.K. Cho, J.H. Kim. *J. Pharm. Biomed. Anal.*, **12**, 157 (1994).
[82] R.C. Li, D.E. Nix, J.J. Schentag. *Pharm. Res.*, **11**, 917 (1994).
[83] H.N. Alkaysi, M.H. Abdel-Hay, M. Sheikh-Salem, A.M. Gharaibeh, T.E. Na'was. *Int. J. Pharm.*, **87**, 73 (1992).
[84] C.M. Riley, D.L. Ross, D.V. Velde, F. Takusagawa. *J. Pharm. Biomed. Anal.*, **11**, 49 (1993).
[85] D.L. Ross, C.M. Riley. *Int. J. Pharm.*, **87**, 203 (1992).
[86] I. Turel, N. Bukovec, E. Farkas. *Polyhedron*, **15**, 269 (1996).
[87] P.T. Djurdjevic, M.J. Jelikic-Stankov, D. Stankov. *Anal. Chim. Acta*, **300**, 253 (1995).
[88] R. Jelic, M. Tomovic, S. Stojanovic, L. Joksovic, I. Jakovljevic, P. Djurdjevic. *Monatsh. Chem.*, **146**, 1621 (2015).
[89] F.A. Cotton, G. Wilkinson. *Advanced Inorganic Chemistry, A Comprehensive Text*, Interscience Publishers, New York (1972).
[90] H. Zuyun, H. Houping, C. Ruxin, Z. Yun. *Wuhan Univ. J. Nat. Sci.*, **2**, 353 (1997).
[91] M.E. El-Kommos, G.A. Saleh, S.M. El-Gizawi, M.A. Abou-Elwafa. *Bull. Pharm. Sci.*, **29**, 289 (2006).
[92] H.R. Park, C.H. Oh, H.C. Lee, J.G. Choi, B.I. Jung, K.M. Bark. *Bull. Korean Chem. Soc.*, **27**, 2002 (2006).
[93] A.P. Vilches, M.J. Nieto, M.R. Mazzieri, R.H. Manzo. *Molecules*, **5**, 398 (2000).
[94] K. Kaur, B. Singh, A.K. Malik. *Anal. Lett.*, **44**, 1602 (2011).
[95] P. Gans, A. Sabatini, A. Vacca. *Annali di Chimica*, **89**, 45 (1999).
[96] M. Sakai, A. Hara, S. Anjo, M. Nakamura. *J. Pharm. Biomed. Anal.*, **18**, 1057 (1999).
[97] P. Dervenšek, J. Košmrlj, G. Giester, T. Skauge, E. Sletten, K. Sepčić, I. Turel. *J. Inorg. Biochem.*, **100**, 1755 (2006).
[98] S.A. Sadeek, W.A. Zordok, W.H. El-Shwiniy. *J. Korean Chem. Soc.*, **57**, 574 (2013).
[99] W.R. Harris. *Inorg. Chem.*, **29**, 119 (1990).
[100] Y. Wang, X. Lu, S.Y. Wang, J.F. Han, K.Y. Yang, C.J. Niu, J.Z. Ni. *Chin. Chem. Lett.*, **12**, 161 (2001).
[101] O. Zak, P. Aisen. *Biochemistry*, **27**, 1075 (1988).